International Journal of Information, Control and Computer Sciences
ISSN: 2517-9942
Vol:2, No:4, 2008

Fast Wavelet Image Denoising Based on Local Variance and Edge Analysis

Gaoyong Luo

Abstract**—**The approach based on the wavelet transform has been widely used for image denoising due to its multi-resolution nature, its ability to produce high levels of noise reduction and the low level of distortion introduced. However, by removing noise, high frequency components belonging to edges are also removed, which leads to blurring the signal features. This paper proposes a new method of image noise reduction based on local variance and edge analysis. The analysis is performed by dividing an image into 32 x 32 pixel blocks, and transforming the data into wavelet domain. Fast lifting wavelet spatial-frequency decomposition and reconstruction is developed with the advantages of being computationally efficient and boundary effects minimized. The adaptive thresholding by local variance estimation and edge strength measurement can effectively reduce image noise while preserve the features of the original image corresponding to the boundaries of the objects. Experimental results demonstrate that the method performs well for images contaminated by natural and artificial noise, and is suitable to be adapted for different class of images and type of noises. The proposed algorithm provides a potential solution with parallel computation for real time or embedded system application.

Keywords**—**Edge strength, Fast lifting wavelet, Image denoising, Local variance.

I. Introduction

SCIENTIFIC data sets collected by sensors are generally contaminated with noise, either as a result of the data acquisition process, or because of naturally occurring phenomena such as atmospheric disturbance, which can all degrade the target data of interest [1]. A first pre-processing step in analyzing such data sets is denoising, that is, estimating the unknown signal of interest from the available noisy data.

As multi-dimensional data, an image is often corrupted by noise in its acquisition and transmission [2]. Images acquired through modern sensors, such as charge-coupled device (CCD) cameras, may be contaminated by a variety of noise sources [3]. As a result, an image might be degraded by noise leading to a significant reduction of its quality [4]. Image noise is usually with reference to stochastic variations as opposed to deterministic distortions such as shading or lack of focus. It is actually the degree of variation of pixel values caused by the statistical nature of radioactive decay and detection processes. Even if we acquire an image of a uniform (flat) source on an ideal gamma camera with perfect uniformity and efficiency, the number of counts detected in all pixels of the image will not be the same. In addition to noise added inherently by a sensor, image processing techniques also corrupt the image with noise [5]. Therefore for any sophisticated algorithms in computer vision and image processing, noise reduction is a required step to remove the noise while retaining as much as possible the important signal features. This problem has existed for a long time and yet there is no good enough solution for it [6]. A tradeoff between the removed noise and the blurring in the image always exists. Generally speaking, image noise comes in two parts, luminance noise and chroma noise. Luminance noise makes an image look grainy on screen, but is usually not visible when printed. Chroma noise is visible as random red and blue pixels and is usually less obvious both on screen and printed. Removing luminance noise reduces the sharpness of the image and removing the chroma noise damages some of the correct color. So noise reduction is a balance between how much softness and color damage we are willing to accept versus how much noise we want to remove. Unless using an uncompressed mode with camera, JPEG artifacts also get added into the mix. In many applications, image denoising is used to produce good estimates of the original image from noisy observations. The restored image should contain less noise than the observations while still keep sharp transitions (i.e. edges) [7]. Traditionally, spatial filters, such as mean filter, median filter and wiener filter, have long been used for removing noise from images and signals [2], [8]. These filters, known as linear filtering technique, usually smooth the data to reduce the noise, but, in the process, also blur the data. Edge-preserving smoothing algorithm, such as symmetric nearest neighbor (SNN) filter [9], maximum homogeneity neighbor (MHN) filter [10], and morphology-based filter [11], smoothes noise in homogeneous regions and sharpens the boundaries between regions. However, these methods generally involve the choice of the size and shape of the structuring element (filter window). The size of the structuring element directly influences the degree of noise smoothing by the filter, and the size and shape both affect the preservation of fine details in the image. Recently, there has been a lot of work on nonlinear techniques in various scientific communities that claim to improve on spatial filters by denoising more effectively while better preserving the edges in the data. Among them, nonlinear wavelet-based image denoising methods have attracted extensive research attentions over the last decade [12], [13], because of the multi-resolution

Manuscript received March 15, 2005.

G. Y. Luo is with Faculty of Technology, Buckinghamshire Chilterns University College, Queen Alexandra Road, High Wycombe, Buckinghamshire HP11 2JZ, UK (phone: 44-1494-603012; fax: 44-1494-605051; e-mail: gaoyong.luo@bcuc.ac.uk).

nature, the ability to produce high levels of noise reduction and the low level of distortion introduced. These methods transform the data into a wavelet basis, threshold the wavelet coefficients, then transform back the thresholded coefficients into the original domain to obtain the denoised data. Under certain conditions, the large coefficients in the wavelet domain correspond to the signal features, while the small ones represent mostly noise. One obtains different denoisers depending on the wavelet transform, the number of multiresolution levels, the thresholding function (which specifies how to apply the threshold to the wavelet coefficients), the thresholding rule (which specifies how to calculate the threshold), and in certain cases, the noise estimate (which specifies how to estimate the usually known level of the noise) used. Much of the literature thus far has concentrated on developing adaptive scheme to estimate the best threshold [14]-[16]. Image denoising using various wavelet thresholding or shrinkage schemes has shown to have near-optimal properties in the minimax sense and perform well in simulation studies [17]-[20]. Using the mean squared error (MSE) as a measure of the quality of denoising, the test results show that SureShrink [21] and BayesShrink [22] methods consistently outperform the other wavelet-based technique. However, while the wavelet transform-threshold-inverse transform methods have been successful over extensive tests, the assumption that one can distinguish noise from signal solely based on coefficient magnitudes is violated when noise levels are higher than signal magnitudes. Under this high noise circumstance, the spatial configuration of neighboring wavelet coefficients can play an important role in noise-signal classifications. Signals tend to form meaningful features (e.g. edges), while noisy coefficients often scatter randomly [13]. On the other hand, wavelet-based approaches sometimes create noticeable artifacts that can substantially degrade the image [18].

All denoising algorithms reviewed are some form of a low pass filter. The assumption is that noise is captured by the high frequency coefficients and by filtering these coefficients the unwanted noise is removed. Unfortunately, edges also have high frequency components and by removing noise, high frequency components belonging to edges are also removed [23]. While spatial filters are very simple to implement and computationally faster than wavelet-based methods [18], they often result in grainier images than the ones obtained from wavelet techniques, which generally tend to smooth the edges as well. This paper proposes a new method of wavelet thresholding for image denoising based on local variance and edge analysis to preserve edges.

II. Wavelet Analysis and the Lifting Scheme

The wavelet transform (WT) is a relatively new tool for carving up functions, operators, or data, into components of different frequency, allowing one to study each component separately. Unlike Fourier transform which is an excellent tool for decomposing a signal or function in terms of its frequency components, but not localized in time (space), wavelet transform is known to be more suitable for nonstationary signals where the description of the signal involves both time (space) and frequency. The values of the time frequency representation of the signal provide an indication of the specific times at which certain spectral components of the signal can be observed. Wavelet analysis provides a mapping that has the ability to trade off time resolution for frequency resolution and vice versa. It is effectively a mathematical microscope, which allows the user to zoom on features of interest at different scales and locations.

The WT is defined as the inner product of the signal $x(t)$ with a two-parameter family with the basis function:

$$WT(b,a) = \left\langle x, \Psi_{b,a} \right\rangle = |a|^{-\frac{1}{2}} \int_{-\infty}^{+\infty} x(t) \overline{\Psi}\left(\frac{t-b}{a} \right) dt \qquad (1)$$

where $\Psi_{b,a} = \Psi\left(\frac{t-b}{a} \right)$ is an oscillatory function,

$\overline{\Psi}$ denotes the complex conjugate of Ψ,
b is the time delay (translate parameter) which gives the position of the wavelet,
a is the scale factor (dilation parameter) which determines the frequency content.

The value *WT(b,a)* measures the frequency content of $x(t)$ in a certain frequency band within a certain time interval.

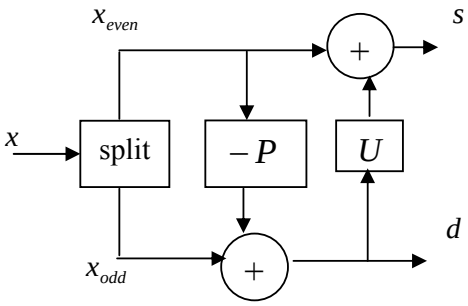

Fig. 1 An example of block diagram of lifting steps

Over the last decade wavelets attracting thousands of theoreticians and engineers both from mathematical analysis and the signal processing community have been applied successfully in such diverse fields as digital communications, remote sensing, vibration, biomedical signal processing, medical imaging, astronomy and numerical analysis. Typical applications include compression, noise reduction, and feature extraction in sound, image, and video processing. The need for improvement of wavelets comes from a shortcoming that is inherent because of its construction. Second generation wavelets named when the concept of lifting was introduced [24], [25], open a new direction to construct wavelets which are not necessarily translates and dilates of one fixed function. A construction using lifting is entirely spatial and therefore ideally suited for building second generation wavelets when Fourier techniques are no longer available. Second generation wavelets are more general in the sense that all the classical

wavelets can be generated by the lifting scheme. The lifting scheme makes optimal use of similarities between the high and low pass filters so as to achieve a faster implementation of wavelet transform. The flexibility afforded by the lifting scheme allows the basis functions associated with wavelet coefficients near a window's boundaries to change their general shape at the boundaries. In this manner, a basis function more accommodating to a boundary can be used to minimize boundary effects. This is the case such as data segmentation where artifacts may be introduced at the boundaries using first generation wavelets with a fixed mother wavelet.

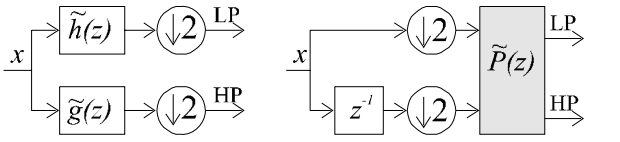

(a) (b)

Fig. 2 An example of forward WT (a) classical case (b) polyphase representation with delay

Lifting steps also known as ladder structures, is a technique to construct wavelet bases or to factor wavelet filters into basic building blocks. An example of block diagram of lifting steps is shown in Fig. 1, where x is a signal, x_{even} is the even part of the signal, and x_{odd} is the odd part, P is a predictor, U is an update operator, and

$$d = x_{odd} - P(x_{even})$$
$$s = x_{even} + U(d) \tag{2}$$

Classical implementation of WT uses two band filter bank (FB) with recursion on its low pass (LP). Equivalent polyphase representation is depicted in Fig. 2, where HP denotes high pass, polyphase matrix $\tilde{P}(z)$ is assembled from even and odd filter components. Output of the FB analysis part is then:

$$\begin{bmatrix} LP \\ HP \end{bmatrix} = \tilde{P}(z) \begin{bmatrix} x_{even} \\ z^{-1} x_{odd} \end{bmatrix} \tag{3}$$

$$\tilde{P}(z) = \begin{bmatrix} \tilde{h}_e(z) & \tilde{h}_o(z) \\ \tilde{g}_e(z) & \tilde{g}_o(z) \end{bmatrix} \tag{4}$$

For any filter pair (h, g) with $\det[P(z)] = 1$, always exist factorisation of $P(z)$ [26]:

$$P(z) = \begin{bmatrix} K & 0 \\ 0 & \frac{1}{K} \end{bmatrix} \prod_{i=m}^{1} \left\{ \begin{bmatrix} 1 & s_i(z) \\ 0 & 1 \end{bmatrix} \begin{bmatrix} 1 & 0 \\ t_i(z) & 1 \end{bmatrix} \right\} \tag{5}$$

Equation (5) allows ladder realization of $\tilde{P}(z)$ by reversible lifting steps followed with normalisation by factor K as shown in Fig. 3.

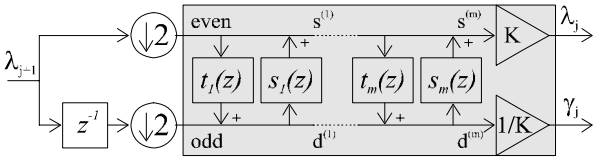

Fig. 3 Ladder structure of lifting steps

Signal is partitioned into even and odd components that are then mutually predicted by t_i (to zero signal in HP part) and updated by s_i (to retain in LP part signal moments). After normalization the algorithm is recursively applied to LP part. Backward transforms simply undo all ladder steps from right to left using reversed operators. Based on the structure of one dimensional (1D) wavelet transform, two dimensional (2D) lifting steps that can be used for predict/update steps on lattices, can then be built for image analysis. The algorithm developed uses weighted coefficients of lifting factorization of 1D prototype transform, but replacing 1D neighborhoods by 2D rings [27]. Weight w_i for lifting coefficient depends on number of pixels in actual ring:

$$w_i = \frac{2}{number\ of\ pixels\ in\ i-th\ ring} \tag{6}$$

Thus filters with forward predict/update steps can be expressed as [27]:

$$d_i^{(st)} = d_i^{(st)} + \sum_k \alpha_k^{(st)} \sum_j nhd_{k,j}\left\{d_i^{(st)}\right\}$$
$$s_i^{(st)} = s_i^{(st)} + \sum_k \beta_k^{(st)} \sum_j nhd_{k,j}\left\{s_i^{(st)}\right\} \tag{7}$$

where st = 1…m (m is number of predict/update steps), $nhd_{k,j}\{center\}$ is operator which returns value of j-th point in k-th neighborhood of *center*, $\alpha_k^{(st)}$ and $\beta_k^{(st)}$ are lifting coefficients associated with actual predict/update step and k-th neighborhood of *center*. New 2D version of forward predict/update steps can be expressed as follows:

$$d_{x,y}^{(st)} = d_{x,y}^{(st)} + \sum_k \alpha_k^{(st)} w_k \sum_j ring_{k,j}\left\{d_{x,y}^{(st)}\right\}$$
$$s_{x,y}^{(st)} = s_{x,y}^{(st)} + \sum_k \beta_k^{(st)} w_k \sum_j ring_{k,j}\left\{s_{x,y}^{(st)}\right\} \tag{8}$$

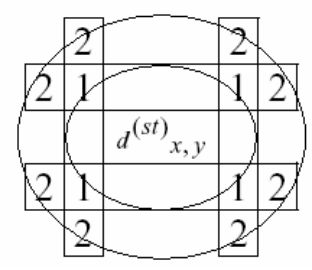

Fig. 4 An example of ring {center}

where $ring_{k,j}\{center\}$ is 2D neighborhood operator as in Equation (7), w_k is weight for k-th ring. An example of ring {center} is shown in Fig. 4 with 4 pixels for the first ring hence $w_1 = 0.5$ and 8 pixels for the second ring hence $w_2 = 0.25$. Thus 2D versions of many biorthogonal filters can be constructed. To implement them, the parameters $\alpha_k^{(st)}$ and $\beta_k^{(st)}$ need to be calculated. In this study, for image decomposition and reconstruction in spectral bands, symmetric biorthogonal wavelet is required for perfect reconstruction. Thus 9/7 filter pair for fast computation is used by factoring wavelet transform into lifting steps [28]. This filter pair is smooth and relatively short. The analysis low pass filter has 9 coefficients, while the synthesis high pass filter has 7 coefficients. The mathematical property of symmetry and compact support with 4 vanishing moments in both analysis and synthesis high pass filters, provides the advantages of 9/7 filter bank over other wavelet families in many applications. This is particularly suited to spatial-frequency analysis and feature extraction of image data due to the fast computation and good approximation properties. The factoring process of 9/7 filter pair starts from the analysis filter

$$\tilde{h}_e(z) = h_4(z^2 + z^{-2}) + h_2(z + z^{-1}) + h_0$$

and

$$\tilde{h}_o(z) = h_3(z^2 + z^{-1}) + h_1(z + 1) \quad (9)$$

The lifting coefficients can be computed as

$$r_0 = h_0 - 2h_4h_1/h_3$$
$$r_1 = h_2 - h_4 - h_4h_1/h_3$$
$$s_0 = h_1 - h_3 - h_3r_0/r_1$$
$$t_0 = r_0 - 2r_1$$

The 2D wavelet transform can then be implemented with boundary effects minimized using:

$$\alpha_1^{(1)} = h_4/h_3 = -1.586134342$$
$$\beta_1^{(1)} = h_3/r_1 = -0.0529801185\ 4$$
$$\alpha_1^{(2)} = r_1/s_0 = 0.8829110762$$
$$\beta_1^{(2)} = s_0/t_0 = 0.4425068522$$
$$K = t_0 = 1.149604398$$

An example of image spatial-frequency decomposed in 3 levels is shown in Fig. 5.

III. Wavelet Denoising by Local Variance and Edge Analysis

Wavelet thresholding is a powerful tool for the reduction of noise in images, due to wavelets capability to give detail spatial-frequency information. This property promises a possibility for better discrimination between the noise and the real data. In order to predict or estimate the noise visibility for a given image, it is important to determine a well-defined functional relationship between the image and noise descriptors. In the case of direct observations of the object f, the wavelet transform of the data results in coefficients $\{d_\lambda\}$ of the form [29]

$$d_\lambda = < f, \Psi > + \sigma z_\lambda \quad (10)$$

where d_λ wavelet coefficients
Ψ wavelet function
f object

$\{z_\lambda\}$ represents a Gaussian white noise process, due to the orthonormality of the underlying wavelets. Specifically, by taking the wavelet transform of the data, we obtain a representation which contains the main structure of the image in a relatively few large coefficients, and the noise in the remaining small coefficients. This is because in most cases, noise can generally be represented as a normally distributed (Gaussian), zero-mean random process. Image denoising using various wavelet thresholding or shrinkage schemes, such as SureShrink [21] and BayesShrink [22], is thus performed by thresholding the small wavelet coefficients. The thresholds are derived under certain rules (e.g. universal) and generalized to images in either level- or subband-dependent manner. However, when the thresholding calculated globally applied to the subband or level based wavelet coefficients of an image, and filtering out the small coefficients to remove noise, high frequency components belonging to edges are also removed, which leads to blurring the signal features. To improve wavelet denoising, local variance evaluation can be used. This is because the local variance can effectively characterize the local feature of the image. An area with the smallest variation represents a homogeneous region, while regions containing edges will have a higher variance than more homogeneous regions. In order to effectively reduce image noise, edges or borders between the different domains containing important features for the interpretation of images should be preserved. Here we propose a new denoising method by dividing an image into 32 x 32 pixel blocks and each block is transformed into wavelet domain. The choice of block size is critical. To take advantage of local analysis, block size tends to be small. However too small size does not allow wavelet decomposition in enough levels required by wavelet analysis. The size of 32 is a balance having maximum 4 level spatial-frequency

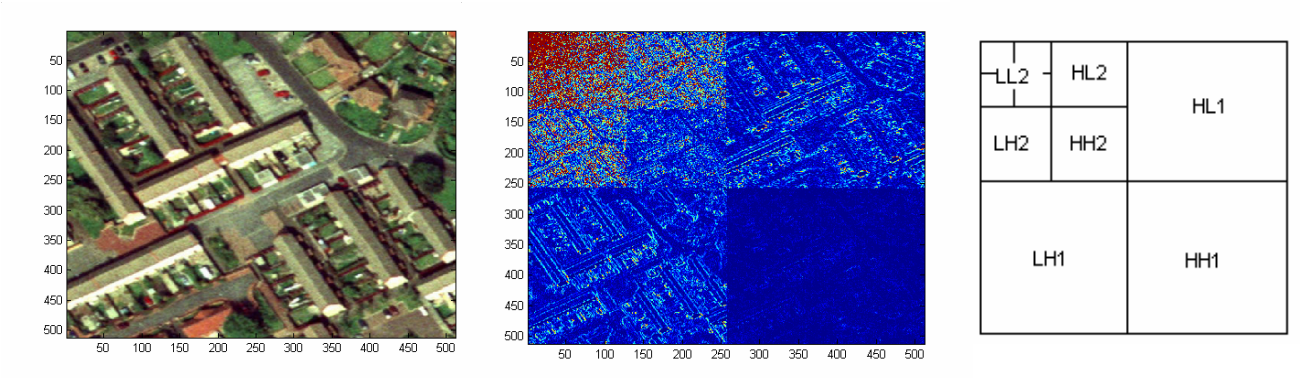

Fig. 5 An aerial image and its spatial-frequency decomposition in 3 levels (bottom right to top left corresponding to high to low frequency subbands)

decomposition that many applications use. Local variance and edge analysis is based on the block in wavelet and image domain. Fast lifting wavelet algorithm is developed for the purpose of spatial frequency decomposition and reconstruction by lifting factorization of the conventional wavelet. The development of fast lifting wavelet transform and inverse transform not only speeds up the calculation, but also minimises the boundary effects. This allows a soft-thresholding scheme to be implemented to threshold the small wavelet coefficients considered to be noise not affecting edges with a subband-dependent noise estimation technique. This thresholding is subband-dependent and can be obtained based on the calculation of noise level, local variance and edge strength. Thus the formula for the threshold on a given subband *j* is:

$$\lambda_j = \eta \frac{20}{\varepsilon} \frac{\hat{\sigma}^2}{\hat{\sigma}_X} \tag{11}$$

where η is a weighting coefficient ($0 < \eta < 100\%$) calculated by the overall noise level estimation [30], ε is the measure of the image edge strength , $\hat{\sigma}^2$ is the local estimated noise variance, and $\hat{\sigma}_X{}^2$ is the local estimated signal variance on the subband considered. The noise variance is estimated as the median absolute deviation of the diagonal detail coefficients on level 1 (highest frequency subband HH_1 16 x 16 block) [22]:

$$\hat{\sigma} = \frac{Median(|W_{ij}|)}{0.6745}, \quad W_{ij} \in subband\ HH_1 \tag{12}$$

The estimate of the signal standard deviation is

$$\hat{\sigma}_X = \sqrt{\max(\hat{\sigma}_W{}^2 - \hat{\sigma}^2, 0)} \tag{13}$$

where $\hat{\sigma}_W{}^2 = \frac{1}{n^2} \sum_{i,j=1}^{n} W_{ij}{}^2$, $\hat{\sigma}_W{}^2$ is an estimate of the variance of the observations, with $n \times n$ being the size of the wavelet coefficients on the subband under consideration. In case $\hat{\sigma}^2 \geq \hat{\sigma}_W{}^2$, all coefficients from the subband are set to zero. The local edge strength is measured by using image gradient [31]:

$$\varepsilon = \frac{1}{32*32}\left[\sum_{i=1}^{31}\sum_{j=1}^{32}|f(i,j) - f(i+1,j)| - \sum_{i=1}^{32}\sum_{j=1}^{31}|f(i,j) - f(i,j+1)|\right] \tag{14}$$

where $f(i,j)$ is image pixel value. The measure indicates how busy the image is in terms of the number of edges and contours in it.

Variance and edge measure are locally computed at each block. Adaptive wavelet denoising is treated in each subband level. The thresholding is governed by the global noise estimation to recognize the real noise coefficients, and to avoid significantly blurring the images, while smooth the noise including that attached to edges. A block with more edges will have a lower threshold value, so that edges can be preserved. Conversely a block with fewer edges will have a higher threshold value, so that more noise can be removed in such a relatively homogeneous region. To illustrate the properties of the proposed noise reduction technique with wavelet thresholding, a 1D example is shown in Figure 6 with noisy signal consisting of sharp changes. The block size used for denoising is 32. The original signal and denoised signal are plotted together for comparison. It can be seen that noises are effectively smoothed while signal features (sharp changes) are well preserved.

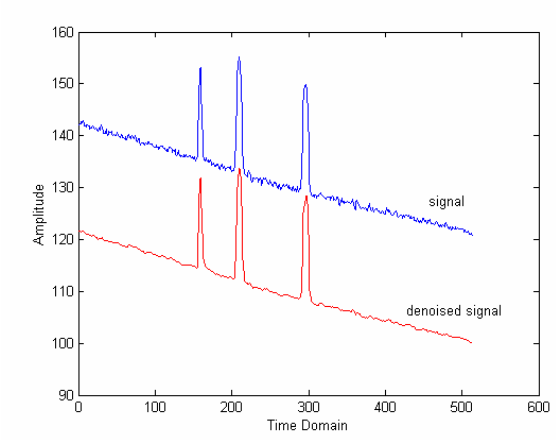

Fig. 6 Noise reduction of 1D example by lifting wavelet thresholding based on local variance and edge analysis

IV. Experimental Results and Discussions

An adaptive fast lifting wavelet thresholding based on local variance and edge analysis was developed for image noise reduction with edge preservation. The proposed algorithm takes the advantage of the development of 2D lifting wavelet by the fast computation and the minimized boundary effects. Hence an image can be divided into 32 x 32 pixel blocks for local variance and edge analysis. The algorithm can be implemented by the following procedure:

a) Global noise estimation of an image
b) Dividing the image into 32 x 32 blocks
c) Edge strength measurement
d) Wavelet spatial-frequency decomposition
e) Local variance estimation
f) Subband-dependent locally adaptive thresholding
g) Wavelet reconstruction
h) Repeat procedure c) to g) for all blocks
i) Image reconstruction with noise reduced

To demonstrate this approach, a standard Lena image was used. The quality of the denoising can be objectively evaluated using the mean squared error (MSE) and the peak signal-to-noise-ratio (PSNR) defined below. For a given estimate $\hat{f}(i, j)$ of $f(i, j)$, the MSE is

$$MSE = \frac{1}{IJ} \sum_{i=1}^{I} \sum_{j=1}^{J} (f(i, j) - \hat{f}(i, j))^2 \quad (15)$$

The PSNR on dB scale is

$$PSNR = 10 \log_{10} \frac{[\max(f(i, j))]^2}{MSE} \quad (16)$$

Fig. 7 shows the denoising results using the Lena image with additive Gaussian noise at standard deviation $\sigma = 15$ (noise level). For visual quality inspection, the best linear filtering technique i.e. wiener filter was also used for comparison. Notice that wavelet thresholding method (BayesShrink) is better than wiener filtering in terms of mean squared error (MSE), but the proposed method is the best, not only because the MSE is smaller, but also the edges are better retained. This can be seen in detail zoom-in images as shown in Fig. 8. It is worth noting that, blocking artifacts is not noticeable as block boundary effects are minimized by changing wavelet shape at the boundaries. Ringing artifacts do not occur around the sharp edges, as the wavelet thresholding is dependent on the edge strength. For comparison, a stronger noise level with $\sigma = 40$ and block size of 64 were also used for testing the denoising methods. The denoising results are summarized in Table I. The choice of block size of 32 is justified from the results of best performance of local analysis method. Results in Table I show that the proposed method with block size 32 and 64 both outperforms wiener filter and wavelet thresholding in terms of MSE and PSNR. The noise in these images was artificially added. Three examples are given here using sensor captured (remotely sensed) aerial images with natural noise and stored in JPEG format. The first one with high noise level and the denoised image is shown in Fig. 9. The second one with low noise level and the denoised image is shown in Fig. 10. The third one is a good quality image and the denoised image is shown in Fig. 11. As for sensor image with natural noise, no reference image is available, visual observation is thus used for quality examination. It is noted here that the original image in (A) was corrupted by noise. The test results are illustrated using (B) wiener filtering, (C) wavelet thresholding, (D) wavelet thresholding by local variance and edge analysis. The proposed algorithm produced better result by smoothing the image without blurring edges. It can be seen that the noise in the denoised images is significantly reduced using the proposed approach, while the sharpness is almost unchanged, i.e. the sharp edges are well preserved. To evaluate the computational load, a standard 512 x 512 pixel size image was used and the proposed algorithm was implemented on a Pentium 4 2.0 GHz PC workstation, and the computing time was estimated approximately 25 seconds.

Experimental work has demonstrated that wavelet denoising is more effective than the traditional spatial filter. While the proposed method with fast lifting wavelet thresholding based on local variance and edge analysis is computationally efficient and achieves better denoising results than others. The method performs well both visually and in terms of MSE and PSNR for images contaminated by natural and artificial noise, and is suitable to be adapted for different class of images and type of noises. Although performed serially here, the computations can be massively parallelized.

(a) (b)

(c) (d)

Fig. 7 Denoising results: (A) Lena image with additive Gaussian noise (MSE=285.72) (B) Wiener filter denoising (MSE= 58.83) (C) Wavelet thresholding (MSE=54.39) (D) Wavelet thresholding by local variance and edge analysis (MSE=53.51)

(a) (b) (c) (d)

Fig. 8 Detail zoom-in images corresponding to Fig. 7

TABLE I
COMPARISON OF DENOISING RESULTS OF NOISY LENA IMAGE USING DIFFERENT METHODS

	Noise Level $\sigma = 15$		Noise Level $\sigma = 40$	
Denoising Method	MSE	PSNR	MSE	PSNR
Noisy Image	285.72	23.57	1425.23	16.59
Wiener Filter	58.83	30.43	239.36	24.34
Wavelet Thresholding	54.39	30.78	223.98	24.63
Wavelet Thresholding by Local Analysis (32x32)	53.51	30.85	213.53	24.84
Wavelet Thresholding by Local Analysis (64x64)	54.03	30.81	219.89	24.71

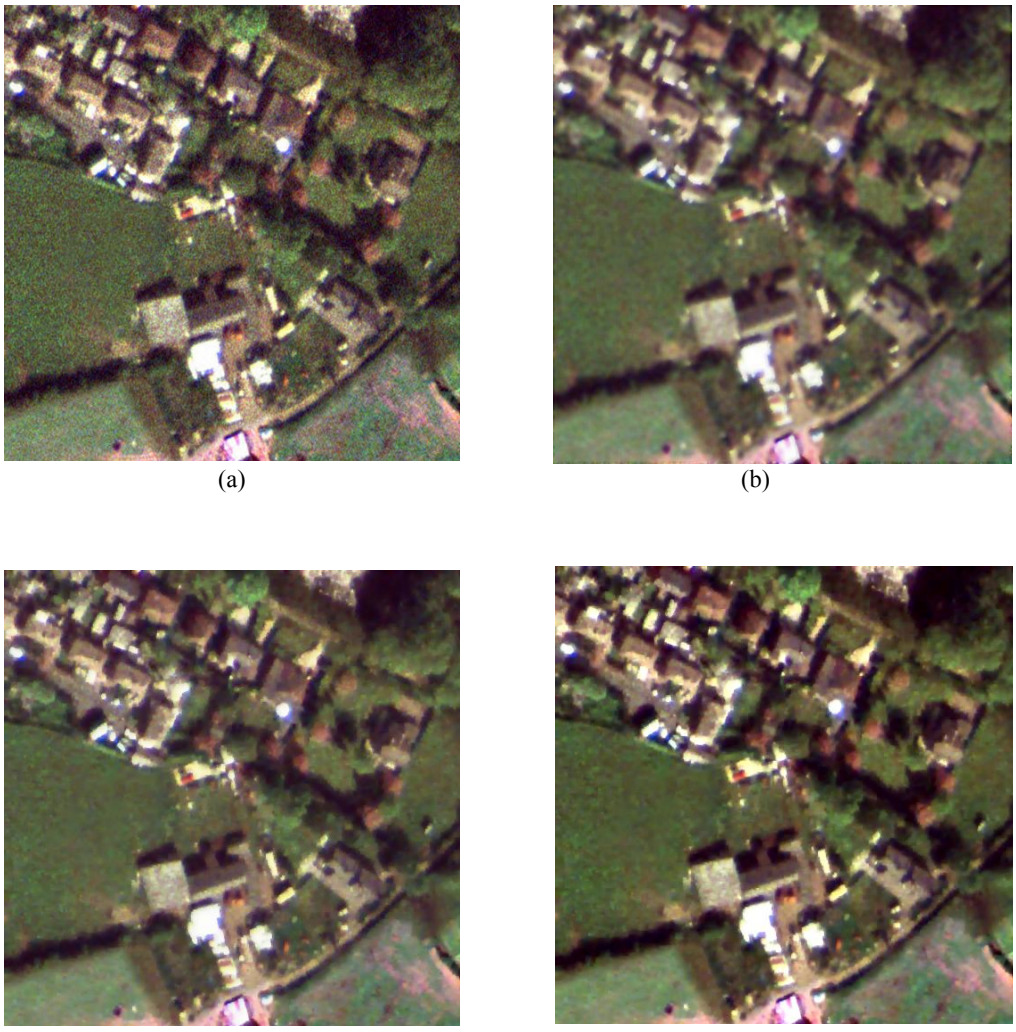

(a) (b) (c) (d)

Fig. 9 Denoising results: (a) Original image (b) Wiener filter denoising (c) Wavelet thresholding (d) Wavelet thresholding by local variance and edge analysis

V. Conclusion

A fast lifting wavelet thresholding based on local variance analysis and edge strength measurement was developed for image noise reduction. Fast lifting wavelet transform for image spatial-frequency decomposition and reconstruction has the advantages of being computationally efficient with boundary effects minimized. The locally adaptive wavelet thresholding scheme is employed to smooth image noise, while still preserve the sharp edges. Experimental results demonstrate that the method performs well both visually and in terms of mean squared error for images contaminated by natural and artificial noise, and is suitable to be adapted for different class of images and type of noises. The proposed algorithm provides a potential solution with parallel computation for real time or embedded system application.

(a) (b)

(c) (d)

Fig. 10 Denoising results: (a) Original image (b) Wiener filter denoising (c) Wavelet thresholding (d) Wavelet thresholding by local variance and edge analysis

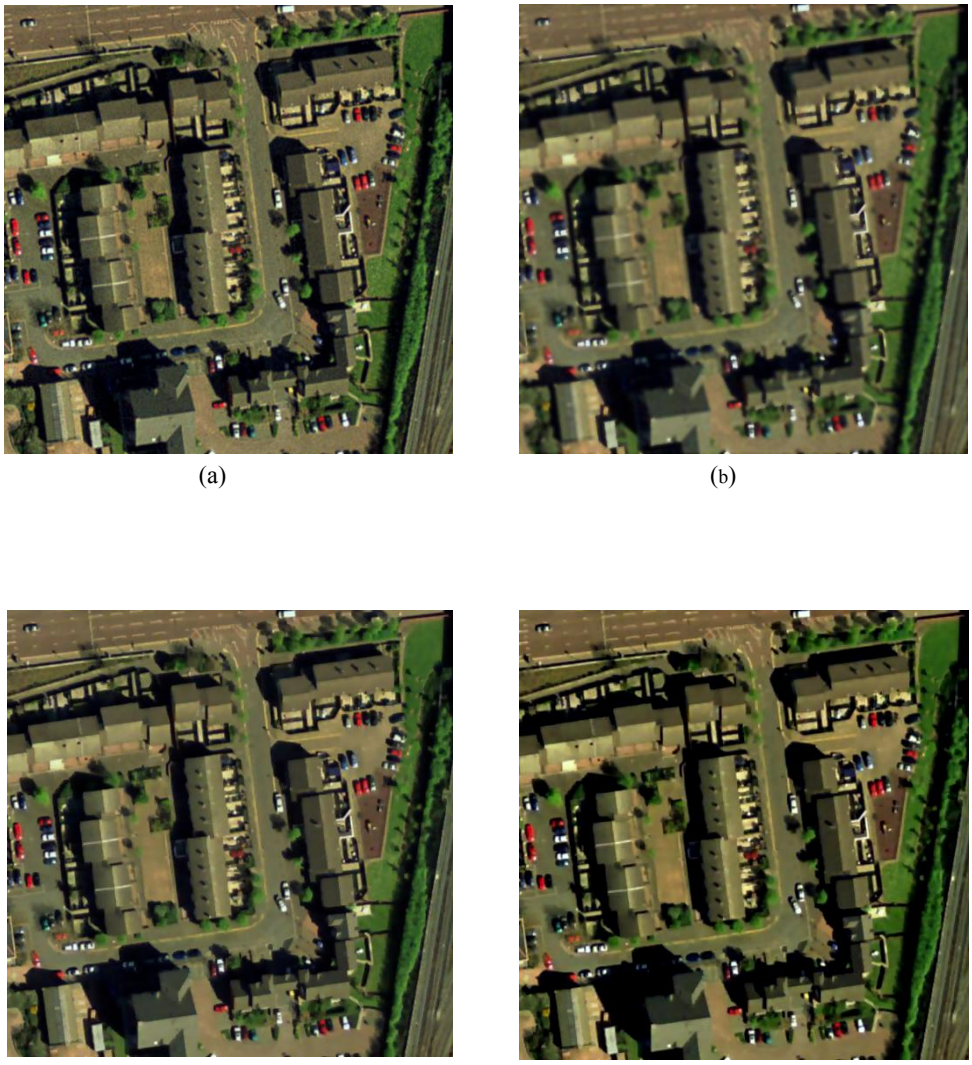

Fig. 11 Denoising results: (a) Original image (b) Wiener filter denoising (c) Wavelet thresholding (d) Wavelet thresholding by local variance and edge analysis

REFERENCES

[1] I. K. Fodor, and C. Kamath, "On denoising images using wavelet-based statistical techniques," Lawrence Livermore National Laboratory LLNL technical report, UCRL JC-142357, 2001.

[2] I. Pitas, *Digital Image Processing Algorithms and Applications*, John Wiley & Sons, Inc., 2000.

[3] Z. Devcic, and S. Loncaric, "SVD block processing for non-linear image noise filtering," *Journal of Computing and Information Technology*, Volume 7, Number 3, pp 255-259, 1999.

[4] S. Voloshynovskiy, O. Koval, and T. Pun, "Wavelet-based image denoising using non-stationary stochastic geometrical image priors," in: *Proceedings of SPIE Photonics West, Electronic Imaging 2003, Image and Video Communications and Processing V*, Santa Clara, CA, USA, January 20-24, 2003.

[5] S.K. Ponnappan, R.M. Narayanan, and S.E. Reichenbach, "Effects of uncorrelated and correlated noise on image information content," in: *Proceedings of the International Geoscience and Remote Sensing Symposium*, Sydney, Australia, 2001, pp. 1898-1900.

[6] A. Gyaourova, C. Kamath, and I. K. Fodor, "Undecimated wavelet transforms for image de-noising," Lawrence Livermore National Laboratory LLNL technical report, UCRL-ID-150931, 2002.

[7] S. Zhong, and V. Cherkassky, "Image denoising using wavelet thresholding and model selection," in: *Proceedings of the IEEE International Conference on Image processing*, vol.3, Vancouver, BC, Canada, 2000, pp 262-265.

[8] A.R. Weeks, *Fundamentals of Electronic Image Processing*, SPIE Optical Engineering Press and IEEE Press, 1996.

[9] D. Harwood, M. Subbararao, H. Hakalahti, and L. Davis, "A new class of edge preserving smoothing filters," *Pattern Recognition Letters*, 5:155–162, 1987.

[10] C. Garnica, F. Boochs, and M. Twardochlib, "A new approach to edge-preserving smoothing for edge extraction and image segmentation," in: *Proceedings of International Archives of Photogrammetry and Remote Sensing*, IAPRS Symposium, Amsterdam, The Netherlands, 2000.
[11] M. A. Schulze, and J. A. Pearce, "A morphology-based filter structure for edge-enhancing smoothing," in: *Proceedings of the 1994 IEEE International Conference on Image Processing*, ICIP-94, Austin, Texas, 13-16 November, 1994, pp. 530-534.
[12] D. L. Donoho, and I. M. Johnstone, "Ideal spatial adaptation via wavelet shrinkage," *Biometrika*, vol. 81, pp. 425–455, 1994.
[13] L. Fan, L. Fan, and C. Tan, "Wavelet diffusion for document image denoising," in: *Proceedings of the Seventh International Conference on Document Analysis and Recognition*, Volume II, Edinburgh, Scotland, 2003.
[14] S. Chang, B. Yu, and M. Vetterli, "Image denoising via lossy compression and wavelet thresholding," in: *Proceedings of the IEEE International Conference on Image Processing*, Washington, DC, October 26-29, 1997, pp 604–607.
[15] S. Chang, B. Yu, and M. Vetterli, "Spatially adaptive wavelet thresholding with context modeling for image denoising," in: *Proceedings of the IEEE International Conference on Image Processing*, Chicago, Illinois, October 04 - 07, 1998, pp 535–539.
[16] D. L. Donoho, "De-noising by soft-thresholding," *IEEE Trans. Inform. Theory*, vol. 41, pp. 613–627, 1995.
[17] S. Chang, B. Yu, and M. Vetterli, "Spatially adaptive wavelet thresholding with context modeling for image denoising," *IEEE Transactions on Image Processing*, Vol. 9, No. 9, pp 1522-1531, 2000.
[18] I.K. Fodor, and C. Kamath, "Denoising through wavelet shrinkage: an empirical study," *Journal of Electronic Imaging*, Volume 12, Issue 1, pp. 151-160, 2003.
[19] M.K. Mihcak, I. Kozintsev, K. Ramchandran, and P. Moulin, "Low-complexity image denoising based on statistical modeling of wavelet coefficients," *IEEE Signal Process. Lett.* 6 (12), pp 300–303, 1999.
[20] D. Cho, and T. D. Bui, "Multivariate statistical modeling for image denoising using wavelet transforms," *Signal Processing: Image Communication* 20 , pp 77–89, 2005.
[21] D. L. Donoho, and I. M. Johnstone, "Adapting to unknown smoothness via wavelet shrinkage," *Journal of the American Statistical Assoc*., vol. 90, no. 432, pp.1200–1224, 1995.
[22] S. Chang, B. Yu, and M. Vetterli, "Adaptive wavelet thresholding for image denoising and compression," *IEEE Transactions on Image Processing*, Vol. 9, No. 9, 1532-1546, 2000.
[23] D. D. Muresan, and T. W. Parks, "Adaptive principal components and image denoising," in: *Proceedings of IEEE International conference on Image processing*, Vol. 1, Barcelona, Spain, 14-17 September, 2003, pp 101-104.
[24] W. Sweldens, "The lifting scheme: A custom-design construction of biorthogonal wavelets," *Appl. Comput. Harmon. Anal.* 3(2), 186-200, 1996.
[25] W. Sweldens, "The lifting scheme: A construction of second generation wavelets," *SIAM J. Math. Anal.* 29(2), 511-546, 1998.
[26] I. Daubechies, and W. Sweldens, "Factoring wavelet transforms into lifting steps," *J. Fourier Anal. Appl*. 4(3), 247-269, 1998.
[27] R. Vargic, "An approach to 2D wavelet transform and its use for image compression," *Radioengineering*, Vol. 7, No. 4, 1-6, 1998.
[28] A.R. Calderbank, I. Daubechies, W. Sweldens, and B. Yeo, "Wavelet transforms that map integers to integers," *Appl. Comput. Harmon. Anal.* 5(3), 332-369, 1998.
[29] A. Aldroubi, and M. Unser, *Wavelets in Medicine and Biology*, CRC Press, Inc., Florida, 1996.
[30] G.Y. Luo, "A novel technique of image quality objective measurement by wavelet analysis throughout the spatial frequency range," Proceedings of SPIE, Vol. 5668 Image Quality and System Performance II, R. Rasmussen, Y. Miyake, Eds, 2005, pp. 173-184.
[31] S. Saha, and R. Vemuri, **"**An analysis on the effect of image features on lossy coding performance**,"** *IEEE Signal Processing Letters*, Volume: 7, pp 104-107, 2000.